Infrared Imaging Video Bolometer with a Double Layer Absorbing Foil

Igor V. MIROSHNIKOV, Artem Y. KOSTRYUKOV and Byron J. PETERSON[1)]

St. Petersburg State Technical University, 29 Politechnicheskaya Str., St. Petersburg, 195251, Russia.

[1)]*National Institute for Fusion Science, 322-6 Oroshi-cho, Toki, 509-5292, Japan*

(Received 30 November 2006 / Accepted 11 August 2007)

The object of the present paper is an infrared video bolometer with a bolometer foil consisting of two layers: the first layer is constructed of radiation absorbing blocks and the second layer is a thermal isolating base. The absorbing blocks made of a material with a high photon attenuation coefficient (gold) were spatially separated from each other while the base should be made of a material having high tensile strength and low thermal conductance (stainless steel). Such a foil has been manufactured in St. Petersburg and calibrated in NIFS using a vacuum test chamber and a laser beam as an incident power source. A finite element method (FEM) code was applied to simulate the thermal response of the foil. Simulation results are in good agreement with the experimental calibration data. The temperature response of the double layer foil is a factor of two higher than that of a single foil IR video bolometer using the same absorber material and thickness.

Keywords: plasma bolometry, infrared imaging bolometer, double layer foil, finite element method simulation

DOI: 10.1585/pfr.2.S1052

1. Introduction

The idea of infrared imaging bolometry is to absorb the incident plasma radiation in an ultra thin (1 μm-2.5 μm) metal foil, to measure the temperature rise of the foil remotely by means of infra red video camera and finally to calculate the incident radiation power flux as a function of the measured temperature rise. Initially [1] metal foil pixels were thermally isolated by two segmented supporting plates. The central part of the plates was later eliminated [2] and a large (10 cm×10 cm) foil was supported by a copper frame. The thermal fluxes between the neighboring pixels were calculated and taken into account during a special reconstruction procedure.

To achieve the most effective transformation of the incident radiation power flux into infrared radiation measured by an infrared camera one should provide good thermal isolation of each bolometer pixel from the other pixels and from the supporting frame. The object of the present paper is a first experimental sample of an infrared video bolometer with a bolometer foil consisting of two layers: radiation absorbing layer and thermal isolating base.

Part 2 describes the double layer foil (DLF) design and manufacturing procedures. Part 3 explains the finite element method used for thermal simulation of the DLF. Part 4 describes the experimental calibration test bench. Part 5 contains a comparison of the FEM simulation and experimental results and discussion. Conclusions and future plans are given in Part 6.

2. Double Layer Foil Design and Manufacturing

The idea of DLF design is shown in Fig. 1.

The first layer contains radiation absorbing blocks made of a material with a high photon attenuation coefficient (gold, platinum). The blocks were spatially separated from each other while the base can be made of a material having high tensile strength and low thermal conductance (stainless steel, havar).

Since the stainless steel SS304 thermal conductivity is 30 times lower than that of gold even a 1 mm wide stainless steel gaps between 5 mm × 5 mm square golden blocks make it possible to decrease the effective thermal conductivity of the foil substantially.

On the other hand the additional heat capacitance of the base layer inevitably delays the thermal response of the DLF to the incident radiation. The base should be therefore made as thin as possible to reduce that delay.

Unfortunately, the heat capacitances (joule/gK) of appropriate base layer materials are higher than that of gold

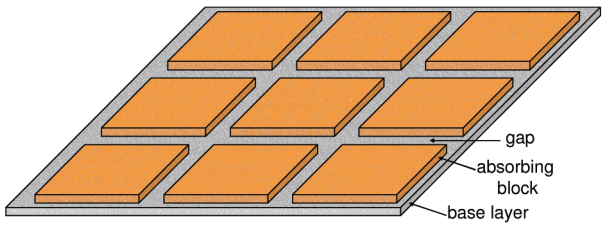

Fig. 1 Double layer foil structure.

author's e-mail: miv-miv@mail.ru

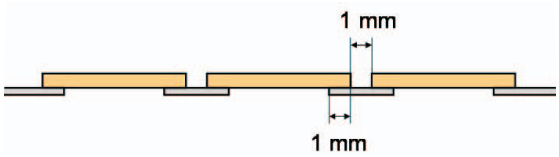

Fig. 2 Cross section of a double layer foil with perforated base.

and platinum. Fortunately, those materials are mechanically much stronger than noble metals, so that the base layer thickness can be reduced to microns at a large foil size. The first prototype used a 100 mm × 200 mm×8 microns SS304 foil. Then the foil was etched down to 2.5 microns using specially developed electrochemical etching technology. The foil thickness has been measured by a mechanical micrometer with an accuracy of ±0.2 micron. At this thickness the foil remained strong enough and could be handled easily. Further improvement of the DLF implies SS foil etching down to 1 micron while the main goal is to avoid etching non-uniformity.

An alternative way to reduce the base layer heat capacitance is to etch away the parts of the base layer which lie beneath the absorbing blocks (see Fig. 2).

Effective electrochemical etching cannot be used for that since it requires the foil to be put onto a special support and submerged into the electrolyte solution. Therefore the foil was installed in a stainless steel frame similar to those used in the IRVB experiments on LHD and the process was performed by a 0.6 keV Argon ion beam patterned by a special mask. The ion beam etching process is slow and needs to be improved.

Gold deposition was done by means of a vacuum evaporation process with the use of a perforated molybdenum mask put in front of the foil. The process makes it possible to vary the thickness of gold across the foil by putting additional covers onto the mask. Gold adhesion to stainless steel is good enough. However careful ion beam cleaning of the surface is needed to avoid gold exfoliation. Thermal strain at the gold/SS interface can be totally relieved by ion beam bombardment as well.

Fig. 3 shows the front (radiation absorbing) side of the DLF prototype. Two golden blocks in the lower left corner exfoliated. The blocks in left half of the foil are 2.1 ± 0.1 microns thick, the gold thickness in the right part is 0.85 ± 0.1 micron. Four blocks in each part of the foil were blackened by carbon spray (0.2-0.4 microns).

Fig. 4 shows the back (IR camera) side of the DLF prototype. The stainless steel base foil underneath the gold absorber blocks was partially etched through the mask. A portion of the etching products was deposited back to the foil under the mask (see the dark pattern). Four blocks in each part of the foil were blackened by carbon spray.

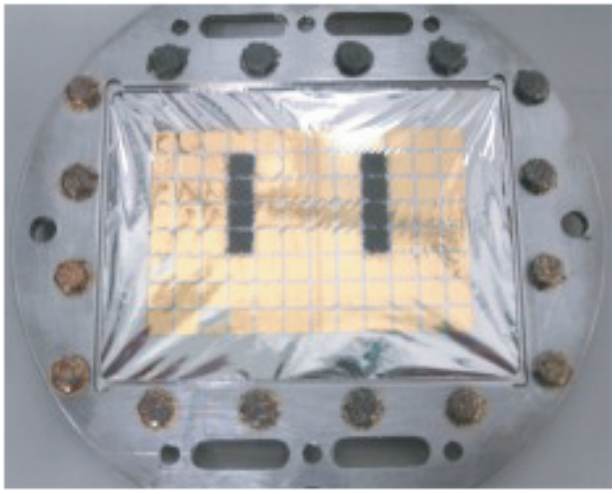

Fig. 3 DLF experimental sample. Front (radiation absorbing) side.

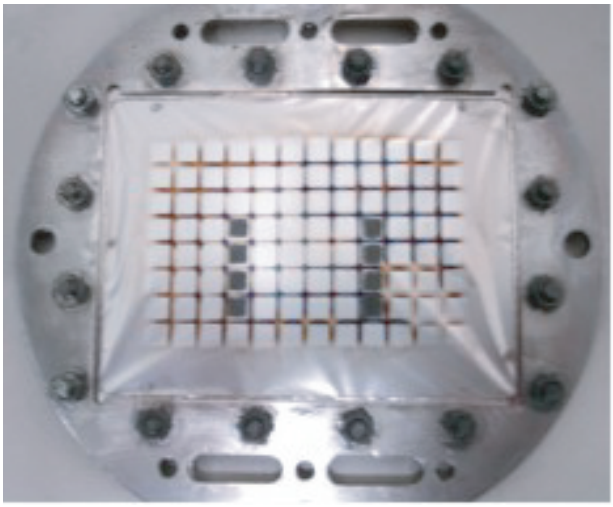

Fig. 4 DLF experimental sample. Back (IR camera viewed) side.

3. Finite Element Method Thermal Simulation of the DLF

The temperature distribution as a function of the incident radiation power can be calculated for a double layer foil using a finite element method calculation.

To ensure good accuracy the element size L should be chosen to be much smaller that the absorbing block size. The time step Δt should be much smaller than the response time of the foil to avoid calculation instability.

The temperature rise of a particular (x, y) element can be calculated as follows:
here

$$\frac{T_{t+1,x,y} - T_{t,x,y}}{\Delta t} = \frac{F_{x,y} + R(T_{t,x,y} - T_r) + \frac{2\lambda_{x,y}\lambda_{x\pm1,y}}{\lambda_{x,y} + \lambda_{x\pm1,y}}(T_{t,x\pm1,y} - T_{t,x,y}) + \frac{2\lambda_{x,y}\lambda_{x,y\pm1}}{\lambda_{x,y} + \lambda_{x,y\pm1}}(T_{t,x,y\pm1} - T_{t,x,y\pm1})}{C_{x,y}}$$

$F_{x,y} = PL^2$ -incident energy flux,
P -incident radiation power flux,
$R = \sigma S(\varepsilon)_f + \varepsilon_b)4T_r^3$ -energy losses due to infrared radiation
$\sigma = 5.67\ 10^{-8}\,\mathrm{W/m^2K^4}$, $\varepsilon_b = 1$ -emissivity of the blackened side of the foil and ε_f -emmisivity of the front side. Since $T - T_r \ll T_r$ a linear approximation can be used:

$$Q_r = \sigma S(\varepsilon_f + \varepsilon_b)(T^4 - T_r^4) \approx \sigma S(\varepsilon_f + \varepsilon_b)4T_r^3(T - T_r))$$

$C_{x,y} = C_{abs}\rho_{abs}L^2h_{a+}C_{waf}\rho_{waf}L^2h_{waf}$ -total heat capacitance of the foil element
C_{abs}, ρ_{abs}, h_a absorbing block heat capacitance coefficient, mass density and thickness.
C_{waf}, ρ_{waf}, h_{waf} -base layer heat capacitance coefficient, mass density and thickness.
$\lambda_{x,y} = (\lambda_{abs}h_{abs} + \lambda_{waf}h_{waf})$ -effective thermal conductance of the foil element
λ_{abs}, λ_{waf} -absorbing block and base layer heat conductance coefficients.
It is assumed that the temperature is 300 K at the moment in time when the radiation flux is switched on.
$T_{x,y} = 300\,\mathrm{K}$ for $t = 0$

The numerical data was taken from the free internet data source [3].

4. Calibration Test Bench

Both the double layer foil and the 2.5 microns golden IRVB foil were calibrated in a vacuum test chamber by a HeNe laser.

The vacuum chamber with the foil installed was evacuated down to < 1 mTorr. Both the DLF and the golden foil thermal response increased by a factor of 2 when the pressure dropped from 100 to 1 mTorr. The effect is likely due to water evaporation from the blackened surface of the foil.

The fast framing 320 × 256 pixels Indigo-Phoenix IR camera by FLIR was calibrated using a thermocouple and installed 1.1 m from the bolometer foil in front of a ZnSe vacuum window. The camera spectral range is 3-5 microns and the temperature resolution is less than 0.5 K. The laser beam was pointed on the opposite side of the foil.

The measured laser beam total power was 18 mW while the beam diameter was approximately 2 mm. Laser beam power and beam profile was measured by standard power meter and beam profiler. A special experiment was done to measure the emissivity of the blackened surface. The metal sample surface was blackened and a black hole was made in the sample to provide an absolute black body radiation (emissivity = 1). The surface emissivity was found to be 0.87-0.88.

Two types of experimental data have been recorded: a single frame IR image and a sequence of images with a frame rate of 400-450 Hz. Single images were used to see the saturated temperature profile across the foil. Sequence data were processed to obtain temperature rise curves responding to the laser beam shutter opening.

5. Results and Discussion

Fig. 5 shows the comparison of the DLF and golden foil temperature responses to the laser shutter opening. The local temperature at the point where the laser beam was pointed has been measured and calculated.

Experimental and simulated spatial temperature profiles across the golden foil are shown in Fig. 6. The same results obtained for the DLF are shown in Fig. 7.

One can see a reasonable agreement between the experimental and simulation results. The difference may be caused by the relatively large size of the finite element (0.5 mm × 0.5 mm) and possible errors in the foil emissivity measurements.

The gaps between the golden absorbing blocks on the back side of the DLF were not blackened. That is why some “low temperature” zones have been observed (see blue line in Fig. 7).

Typical IRVB experimental conditions differ from the calibration procedure described above. The incident radi-

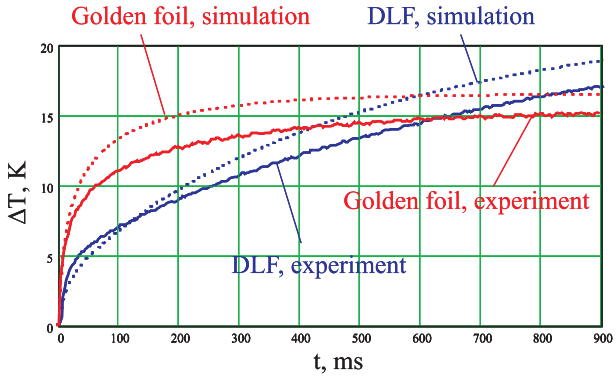

Fig. 5 Thermal response of the DLF and 2.5 microns golden foil to the 18 mW laser beam shutter opening. FEM simulation and experimental data.

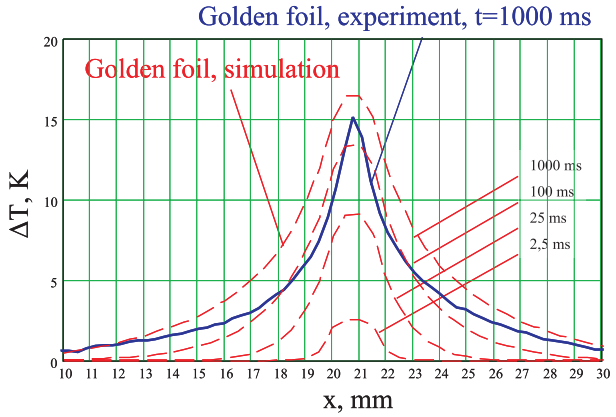

Fig. 6 Time evolution of the golden foil temperature profiles. FEM simulation and experimental data.

ation is not focused in a single point but spread across the whole foil. An additional experiment was done to see the response of the golden foil and the DLF to the wide spread laser beam (laser beam diameter −5 mm).

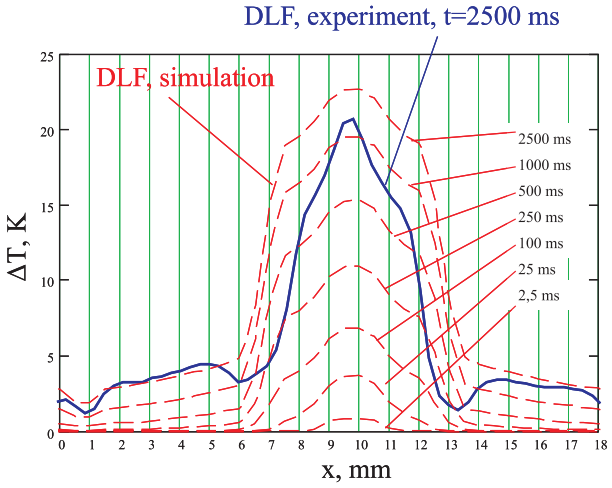

Fig. 7 Time evolution of the DLF temperature profiles. FEM simulation and experimental data.

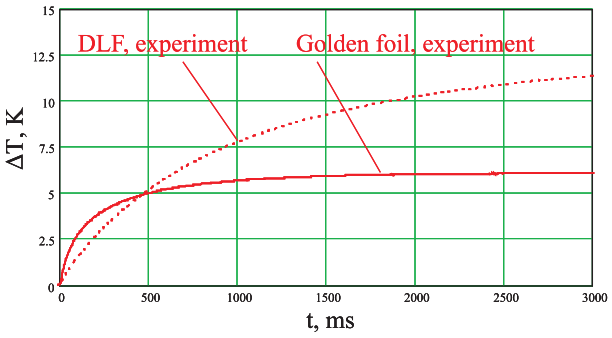

Fig. 8 Thermal response of the DLF and 2.5 microns golden foil to the 14.7 mW laser beam shutter opening, experimental data.

Fig. 8 shows the comparison of the temperature rise curves measured experimentally.

It is seen that the DLF is less sensitive for the signals faster than 500 ms and more sensitive for slow signals. The DLF sensitivity can be further improved by making the base foil thinner (current thickness is 2.5 micron) and/or by etching away the base layer underneath the absorbing blocks.

For ITER applications where the thickness of the gold absorbers should be increased to at least 10 microns [4, 5] the DLF advantage is more sufficient. Let us compare the FEM simulated response of a 10 μm gold/ 2 μm stainless steel DLF and 10 μm golden foil applicable to ITER (see Fig. 9). The fast thermal response of the golden foil and DLF are of the same order of magnitude while the slow thermal response of the DLF is 10 times higher than that of the golden foil.

6. Conclusions

The double layer foil for an infrared video bolometer is a simply produced material which allows us to improve the IRVB sensitivity. A first prototype of the DLF has shown thermal response equal to that of similar golden foil at 500 ms signal rise time. The DLF sensitivity for slow signals is twice better than golden foil sensitivity. Further improvement should be achieved by use of a thinner (1 micron) base foil.

A simple rectangular grid finite element method simulation of the foil response was shown to be an adequate instrument to predict foil thermal properties.

DLF in its present embodiment does not allow a change of the size of the bolometer pixel (part of the foil considered as one bolometer “channel”). The problem can be solved by miniaturizing the DLF pattern. Another DLF drawback is the difference in gold and stainless steel attenuation of high energy photons and particles which may provide slight spectral variations of the bolometer sensitivity.

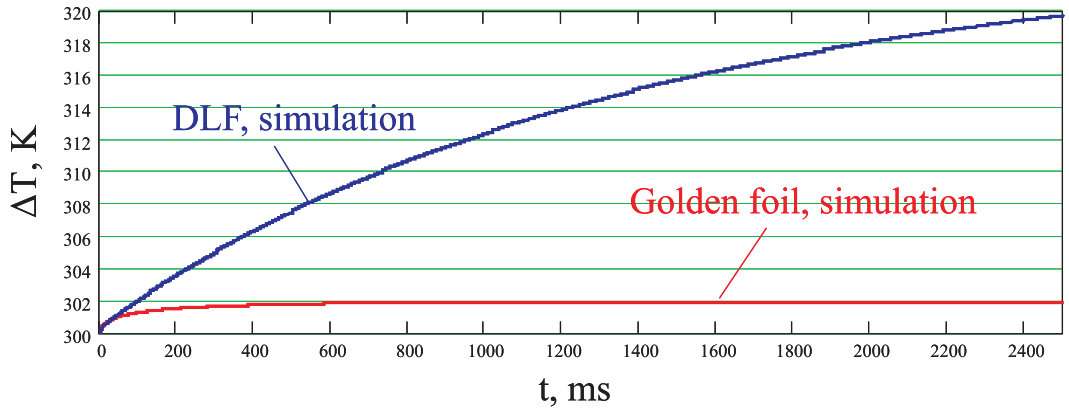

Fig. 9 Thermal response of the 10 μm gold/2 μm stainless steel DLF and 10 μm golden foil to the 14.7 mW/5 mm laser beam shutter opening. FEM simulation.

Acknowledgements

This research is supported by MEXT Grant-in-Aid # 16082207.

[1] G.A. Wurden, B.J. Peterson and S. Sudo, Rev. Sci. Instrum. **68**, 766 (1997).
[2] B.J Peterson, A. Yu. Kostryukov *et al.*, Rev. Sci. Instrum. **74**, 2040 (2003).
[3] www.matweb.com
[4] G.A. Wurden, B.J. Peterson, Imaging Bolometer Development for Large Fusion Devices, 1997 Varenna ITER Diagnostic Workshop, LA-UR-97-3586.
[5] G. Wurden, A rad-hard, steady-state, digital imaging bolometer system for ITER, In Diagnostics for Experimental Thermonuclear Fusion Reactors (Plenum Press, NY, 1996) pp.603-606.